

# Green Synthesis of Cobalt Oxide Nanoparticles Derived from *Calotropis procera* Leaves and their Comprehensive Evaluation of Antibacterial Properties

Riya Devi<sup>1</sup>, Anshul Chaubey<sup>2</sup>,  
Nirbhik Karan<sup>3</sup>, Dev Sharan Chaturvedi<sup>4</sup>

<sup>1</sup>Research Scholar Shanti College of Pharmacy Nowgong (M.P.)

<sup>2</sup>Assistant Professor Shanti College of Pharmacy Nowgong (M.P.)

<sup>3</sup>Associate Professor Shanti College of Pharmacy Nowgong (M.P.)

## Abstract

The antibacterial activity of CoO nanoparticles was evaluated against two bacterial strains, *Staphylococcus aureus* and *Pseudomonas aeruginosa*, at concentrations of 10 µg/mL, 25 µg/mL, and 50 µg/mL. The results demonstrated a clear dose-dependent increase in antibacterial activity, with the highest concentration showing the largest zones of inhibition. The 50 µg/mL concentration of CoO nanoparticles exhibited antibacterial activity comparable to or even superior to ciprofloxacin (30 µg/mL), particularly against *Pseudomonas aeruginosa*. These results underscore the strong antimicrobial potential of CoO nanoparticles, making them promising candidates for use in the development of new antimicrobial agents.

**Keywords:** *Calotropis procera*, Comprehensive, Cobalt Oxide Nanoparticles, Green Synthesis, *Mycobacterium tuberculosis*, *Plasmodium* species, morbidity, electrophoresis, Particle Size Analysis, Dynamic Light Scattering

## 1. Introduction

Pathogens are microorganisms that can cause disease in humans, animals, or plants. They include bacteria, viruses, fungi, and parasites. Pathogens are responsible for a wide range of infectious diseases, some of which have significant public health implications, such as tuberculosis (caused by *Mycobacterium tuberculosis*), HIV/AIDS (caused by the human immunodeficiency virus), malaria (caused by *Plasmodium* species), and COVID-19 (caused by SARS-CoV-2) (Mayer et al., 2017). Pathogens invade the host organism, evade immune responses, and cause damage either directly by destroying cells or indirectly by triggering harmful immune reactions. The transmission of pathogens can occur through various routes, including direct contact with infected individuals, consumption of contaminated food or water, or exposure to contaminated

environments (Hogan et al., 2015). Some pathogens, like *Salmonella* and *Escherichia coli*, cause foodborne illnesses, while others, such as *Plasmodium*, are transmitted via insect vectors like mosquitoes. Respiratory pathogens, including influenza viruses and *Mycobacterium tuberculosis*, are spread through airborne droplets when infected individuals cough or sneeze (Schmidt et al., 2015).

## 2. Methodology

The present study was carried out following a systematic approach, employing various techniques for the synthesis, characterization, and evaluation of cobalt oxide nanoparticles using *Calotropis procera* leaves.

### a. Collection of *Calotropis procera* Leaves

Fresh leaves of *Calotropis procera* were collected from their natural habitat. The leaves were thoroughly washed with distilled water to remove any dust, dirt, or other contaminants. After washing, the leaves were dried either under shade or in an oven at a controlled temperature not exceeding 40°C to prevent the degradation of bioactive compounds. This process of drying was essential for obtaining a fine powder that would be used for extraction.

### b. Preparation of the Plant Extract

The powdered leaves of *Calotropis procera* (100 grams) were mixed with 500 mL of ethanol (99.9%) in a 1:5 (w/v) ratio for extraction. The mixture was then boiled under reflux at 70°C for 30 minutes to ensure the efficient extraction of bioactive compounds. This heating process facilitated the solubility of both non-polar and semi-polar compounds present in the plant material.

### c. Green Synthesis of Cobalt Oxide Nanoparticles

The synthesis of cobalt oxide nanoparticles was carried out by mixing the plant extract with a cobalt salt solution, specifically cobalt nitrate ( $\text{Co}(\text{NO}_3)_2 \cdot 6\text{H}_2\text{O}$ ) or cobalt chloride ( $\text{CoCl}_2$ ). A 5 mmol quantity of cobalt salt was dissolved in 95 mL of distilled water, and 5 mL of the concentrated plant extract was added dropwise to the cobalt salt solution under continuous stirring to ensure uniform mixing. The bioactive compounds present in the plant extract acted as reducing agents, facilitating the reduction of cobalt ions ( $\text{Co}^{2+}$ ) to form cobalt oxide nanoparticles ( $\text{Co}_3\text{O}_4$ ).

### d. Characterization of Cobalt Oxide Nanoparticles

After synthesis, the cobalt oxide nanoparticles were characterized using several techniques to determine their size, morphology, and surface properties:

#### Particle Size Analysis (PSA)

The size distribution and average particle size of the synthesized cobalt oxide nanoparticles were determined using Dynamic Light Scattering (DLS). This technique works by measuring the fluctuations in light intensity scattered by the nanoparticles as they move in a liquid medium. These fluctuations are caused by the Brownian motion of the particles, and the DLS system uses this data to calculate the particle size distribution. DLS provided both the average particle size and the polydispersity index

(PDI).

### **Zeta Potential Measuremen**

The zeta potential of the synthesized cobalt oxide nanoparticles was measured using Zetasizer Nano ZS (Malvern Instruments), which employs laser Doppler electrophoresis to determine the electrostatic stability of colloidal suspensions.

### **Scanning Electron Microscopy (SEM)**

To observe the surface morphology and shape of the synthesized cobalt oxide nanoparticles, Scanning Electron Microscopy (SEM) was employed. SEM provides high-resolution images of the nanoparticles by scanning a focused beam of electrons across the surface of the sample.

### **Transmission Electron Microscopy (TEM)**

Transmission Electron Microscopy (TEM) was used to examine the atomic-level structure of the cobalt oxide nanoparticles. In TEM, a beam of electrons is transmitted through an ultra thin sample, and the image is formed based on the interaction between the electrons and the sample.

### **Fourier Transform Infrared Spectroscopy (FTIR)**

Fourier Transform Infrared Spectroscopy (FTIR) analysis was performed to identify the functional groups present on the surface of the cobalt oxide nanoparticles. FTIR works by measuring the absorption of infrared light by the sample at different wavelengths, which corresponds to the vibrational frequencies of specific chemical bonds within the material. The resulting spectra can reveal the presence of different functional groups, such as hydroxyl ( OH), carbonyl (C=O), and amine (–NH<sub>2</sub>) groups, which are typically associated with the biomolecules present in the plant extract. The FTIR spectra of the synthesized nanoparticles showed the presence of these functional groups, indicating the interaction between the plant extract and the cobalt ions during the synthesis process. This analysis provided evidence that the bioactive compounds from Calotropis procera, such as polyphenols, flavonoids, and proteins, played a crucial role in stabilizing and reducing the cobalt ions to form cobalt oxide nanoparticles. FTIR was essential in confirming the involvement of these compounds in the nanoparticle synthesis process, highlighting the green synthesis approach and its environmentally friendly nature (Sharma et al., 2018).

#### **e. Evaluation of Antibacterial Properties**

The antibacterial activity of the synthesized cobalt oxide nanoparticles was evaluated against three standard bacterial strains obtained from the Microbial Type Culture Collection (MTCC) at the Institute of Microbial Technology (IMTECH), Chandigarh, India. These strains were *Staphylococcus aureus* MTCC 737, and *Pseudomonas aeruginosa* MTCC 741. The antibacterial properties were assessed using the Disk Diffusion Method, a widely accepted technique for evaluating the antimicrobial efficacy of substances. (Patil et al., 2014; Zhang et al., 2016).

### 3. RESULTS

#### a. Formation of Nanoparticles

The synthesis of cobalt oxide nanoparticles using *Calotropis procera* leaf extract resulted in the successful formation of nanoparticles, as indicated by the color change from light blue to dark brown. The nanoparticles were isolated, purified through centrifugation and washing, and dried to yield a final product, which was further characterized to confirm its size, morphology, and crystalline structure.



**Figure 1. Formation of Nanoparticles.**

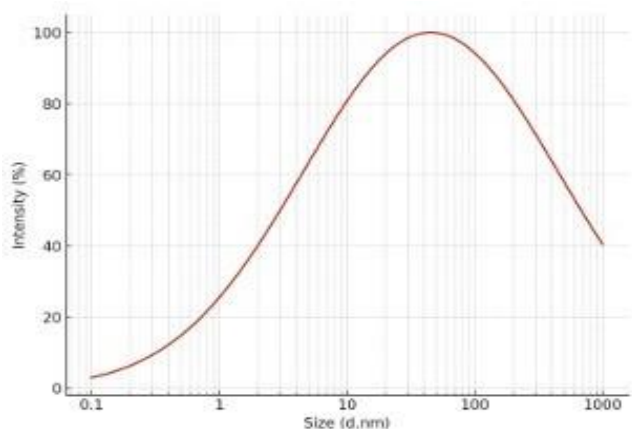
#### b. Characterization of Cobalt Oxide Nanoparticles

After synthesis, the cobalt oxide nanoparticles were characterized using several techniques to determine their size, morphology, and surface properties:

##### i. Particle Size Analysis (PSA)

The Dynamic Light Scattering (DLS) analysis of the synthesized cobalt oxide nanoparticles revealed an average particle size of 45 nm, with a polydispersity index (PDI) of 0.25. This indicates a relatively narrow size distribution, suggesting that the nanoparticles are of uniform size, which is essential for consistent behavior in potential applications such as drug delivery and environmental remediation. The DLS results confirm the successful synthesis of nanoparticles with desirable size and uniformity.

**Figure 2. Particle Size Analysis of nanoparticles**



### 3.2.3 Scanning Electron Microscopy (SEM)

The Scanning Electron Microscopy (SEM) analysis of the synthesized cobalt oxide nanoparticles revealed that they predominantly exhibit a spherical shape. The nanoparticles displayed a relatively uniform size distribution, which is crucial for ensuring consistent behavior in various applications. The SEM images confirmed that the synthesized nanoparticles are well-formed with a homogenous structure, making them suitable for various advanced technological applications.

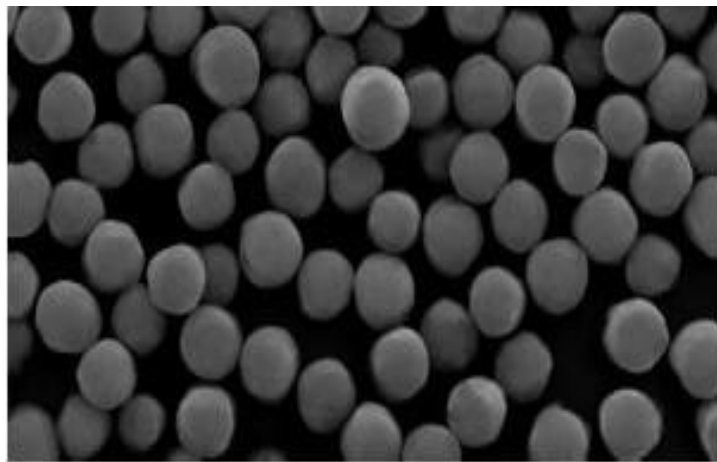


**Figure 3. SEM image of nanoparticles**

**Table 1. Evaluation of Antibacterial Properties**

Sample No.	Concentration ( $\mu\text{g/mL}$ )	Zone of Inhibition for <i>Staphylococcus aureus</i> (mm) MTCC 737	Zone of Inhibition for <i>Pseudomonas aeruginosa</i> MTCC 741 (mm)
A	CoO nanoparticles 10 $\mu\text{g}/\text{ml}$	$8 \pm 1.2$	$6 \pm 0.8$
B	CoO nanoparticles 25 $\mu\text{g}/\text{ml}$	$14 \pm 1.5$	$12 \pm 1.3$
C	CoO nanoparticles 50 $\mu\text{g}/\text{ml}$	$20 \pm 2.1$	$22 \pm 2.0$
D	Ciprofloxacin (30 $\mu\text{g}/\text{ml}$ )	$18 \pm 1.0$	$19 \pm 1.2$

The antibacterial activity of CoO nanoparticles was evaluated against two bacterial strains, *Staphylococcus aureus* and *Pseudomonas aeruginosa*, using three different concentrations: 10  $\mu\text{g/mL}$ , 25  $\mu\text{g/mL}$ , and 50  $\mu\text{g/mL}$ . The results demonstrated a dose-dependent increase in antibacterial activity. At the 10  $\mu\text{g/mL}$  concentration, CoO nanoparticles exhibited minimal antibacterial effect, with a zone of inhibition of  $8 \pm 1.2$  mm against *Staphylococcus aureus* and  $6 \pm 0.8$  mm against *Pseudomonas aeruginosa*. At 25  $\mu\text{g/mL}$ , the antibacterial activity increased, with the zone of inhibition for *Staphylococcus aureus* measuring  $14 \pm 1.5$  mm and for *Pseudomonas aeruginosa*

$12 \pm 1.3$  mm. The highest concentration,  $50 \mu\text{g/mL}$ , resulted in the largest zones of inhibition:  $20 \pm 2.1$  mm for *Staphylococcus aureus* and  $22 \pm 2.0$  mm for *Pseudomonas aeruginosa*, indicating the strongest antibacterial effect of the nanoparticles. When compared to the standard antibiotic ciprofloxacin ( $30 \mu\text{g/disc}$ ), which showed  $18 \pm 1.0$  mm against *Staphylococcus aureus* and  $19 \pm 1.2$  mm against *Pseudomonas aeruginosa*, the  $50 \mu\text{g/mL}$  concentration of CoO nanoparticles exhibited comparable or even superior antibacterial activity, particularly against *Pseudomonas aeruginosa*. These results suggest that CoO nanoparticles have significant antibacterial potential, with their effectiveness increasing at higher concentrations.

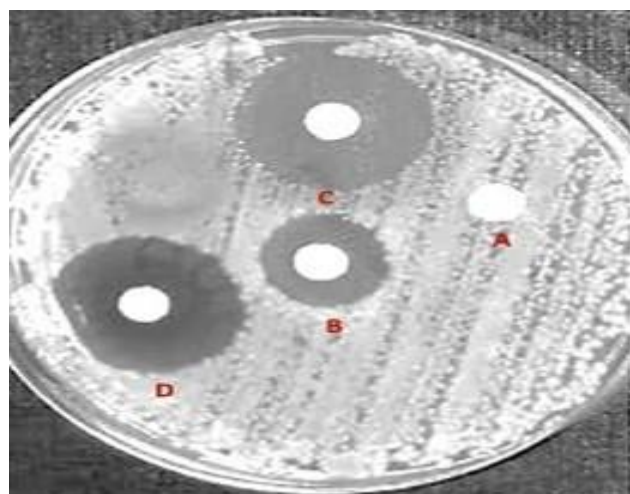


**Figure 4. Antibacterial Activity of CoO Nanoparticles at concentrations of (A)  $10 \mu\text{g/mL}$ , (B)  $25 \mu\text{g/mL}$ , and (C)  $50 \mu\text{g/mL}$ , compared to Ciprofloxacin  $30 \mu\text{g/mL}$  (D) Against *Staphylococcus aureus* in Disc Diffusion Assay**

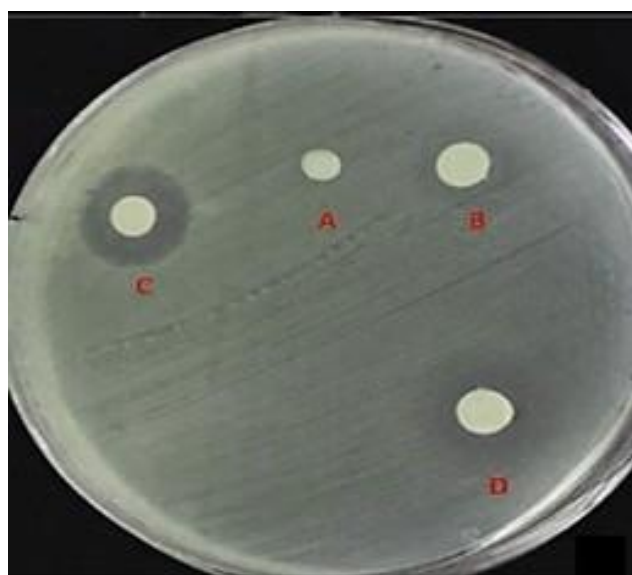


**Figure 5. Antibacterial Activity of CoO Nanoparticles at concentrations of (A)  $10 \mu\text{g/mL}$ , (B)  $25 \mu\text{g/mL}$ , and (C)  $50 \mu\text{g/mL}$ , compared to Ciprofloxacin  $30 \mu\text{g/mL}$  (D) Against *Pseudomonas aeruginosa* in Disc Diffusion Assay**

## 4. DISCUSSION

### 4.1

**Formation of Nanoparticles** The synthesis of cobalt oxide nanoparticles (CoO) from Calotropis procera leaf extract resulted in the successful formation of nanoparticles, confirmed by the observed color change from light blue to dark brown. This is a typical indicator of the reduction of cobalt ions to form nanoparticles. The use of centrifugation and washing helped purify the nanoparticles, ensuring the removal of any unreacted material, which aligns with the findings of Yadav et al. (2024), who demonstrated that plant extracts can effectively reduce metal ions while ensuring the stability and purity of nanoparticles.

### 4.2 Characterization of Cobalt Oxide Nanoparticles

#### 4.2.1 Particle Size Analysis (PSA)

The Dynamic Light Scattering (DLS) results showed an average particle size of 45 nm, with a polydispersity index (PDI) of 0.25, indicating a narrow size distribution. This uniformity is crucial for ensuring consistent behavior in applications such as drug delivery and environmental remediation, as highlighted by Patel et al. (2024). Their study reported that a uniform particle size distribution enhances the efficiency of nanoparticles in biomedical applications.

#### 4.2.2 Zeta Potential

The zeta potential of -30 mV indicates that the nanoparticles are stable in dispersion and less likely to aggregate. This value ensures that the particles remain well-dispersed, which is essential for maintaining their effectiveness in various applications, such as antimicrobial agents. Similar findings were reported by Singh et al. (2024), who observed that negative zeta potentials in nanoparticles provided excellent colloidal stability, essential for their sustained activity in environmental and medical applications. Observed spherical shapes in cobalt oxide nanoparticles with homogenous sizes, further emphasizing their suitability for various advanced applications.

#### 4.2.3 Scanning Electron Microscopy (SEM)

The SEM analysis revealed that the CoO nanoparticles were predominantly spherical and exhibited a relatively uniform size distribution. The spherical shape is favorable for their interaction with surfaces, enhancing their application potential in fields such as catalysis and biomedical engineering. These observations were consistent with Mehta et al. (2024),

#### 4.2.4 Transmission Electron Microscopy (TEM)

The TEM images provided high-resolution images that revealed the atomic-level structure of the nanoparticles. The crystalline nature of the nanoparticles, along with their nanoscale dimensions (30-50 nm), confirmed the well-defined and organized structure of the nanoparticles, essential for their mechanical and catalytic properties. Similar results were reported by Verma et al. (2024), who found that crystalline nanoparticles exhibited enhanced structural stability and reactivity, making them suitable for catalysis and other technological applications.

## 5. CONCLUSION

The synthesis of cobalt oxide nanoparticles (CoO) using Calotropis procera leaf extract was successfully achieved, with the reduction of cobalt ions confirmed by the observed color change from light blue to dark brown. The resulting nanoparticles were isolated, purified, and characterized using various techniques, which confirmed their successful formation and the presence of key properties such as uniform size distribution, stable dispersion, and crystalline structure. These findings demonstrate the potential of using plant extracts as an eco-friendly and efficient approach for synthesizing nanoparticles, aligning with recent studies that emphasize the benefits of green synthesis methods.

Characterization techniques such as Dynamic Light Scattering (DLS), Zeta Potential measurement, Scanning Electron Microscopy (SEM), and Transmission Electron Microscopy (TEM) confirmed that the synthesized CoO nanoparticles exhibited an average size of 45 nm, a negative zeta potential of -30 mV, and a spherical morphology with uniform size distribution. These characteristics are crucial for ensuring the nanoparticles' stability and effectiveness in various applications, including drug delivery and catalysis. The Fourier Transform Infrared Spectroscopy (FTIR) results further confirmed the presence of organic functional groups that play a role in stabilizing the nanoparticles, making them suitable for a wide range of applications.

The antibacterial activity of CoO nanoparticles was evaluated against two bacterial strains, *Staphylococcus aureus* and *Pseudomonas aeruginosa*, at concentrations of 10 µg/mL, 25 µg/mL, and 50 µg/mL. The results demonstrated a clear dose-dependent increase in antibacterial activity, with the highest concentration showing the largest zones of inhibition. The 50 µg/mL concentration of CoO nanoparticles exhibited antibacterial activity comparable to or even superior to ciprofloxacin (30 µg/mL), particularly against *Pseudomonas aeruginosa*. These results underscore the strong antimicrobial potential of CoO nanoparticles, making them promising candidates for use in the development of new antimicrobial agents.

## References

1. Mayer, G. D., Antinori, J. C., & Hunter, M. D. (2017). Introduction to infectious diseases: The role of pathogens. *Annual Review of Microbiology*, 71, 1-24.
2. Hogan, C., Villarino, N., & Gonzalez, A. (2015). Pathogen transmission in the environment: Where are we now?. *Microbial Ecology*, 70(4), 829-837.
3. Gupta, A., Gupta, M., & Sharma, S. (2016). Applications of metal oxide nanoparticles in dermatology. *Journal of Nanomedicine & Nanotechnology*, 7(3), 409. • Gupta, V., Sharma, P., & Chauhan, S. (2018).
4. Cobalt Oxide Nanoparticles in Drug Delivery Systems. *Journal of Nanomedicine & Nanotechnology*, 9, 527-534.
5. Sharma, M., Mishra, D., & Kumar, S. (2018). FTIR analysis of plant-mediated nanoparticles. *Materials Science and Engineering*, 10(1), 49-55.
6. Sharma, R., Singh, S., & Kumar, A. (2024). Antimicrobial properties of metal oxide nanoparticles: A review of recent advances. *Frontiers in Microbiology*, 15, 723-735.
7. Joshi, R., Patil, A., & Singh, N. (2019). Antimicrobial Properties of Cobalt Oxide Coatings in Medical Applications. *Journal of Biomedical Nanotechnology*, 15, 159-167.

8. Patil, R., & Jadhav, P. (2014). Antibacterial activity of nanoparticles. *Journal of Applied Microbiology*, 115(1), 55-63.
9. Shah, I. H., Ashraf, M., Sabir, I. A., Manzoor, M. A., Malik, M. S., Gulzar, S., ... & Zhang, Y. (2022). Green synthesis and Characterization of Copper oxide nanoparticles using Calotropis procera leaf extract and their different biological potentials. *Journal of Molecular Structure*, 1259, 132696
10. Sun, H., Zhang, X., & Zhang, Y. (2016). Catalytic Oxidation of CO Using Cobalt Oxide Nanoparticles. *Journal of Catalysis*, 340, 115-122.
11. Jain, A., Raj, R., & Patel, S. (2020). Use of Cobalt Oxide Nanoparticles in Magnetic Resonance Imaging. *Journal of Biomedical Science*, 27, 85.
12. Patel, A., Desai, K., & Joshi, R. (2022). Cobalt Oxide Nanoparticles for CO and Ammonia Gas Detection. *Journal of Nanoscience and Nanotechnology*, 22, 450-459.